

recognize Cu-PyC in the dimeric form. It is well-known that the dimeric structure and dimer formability of a copper(II) complex are quite dependent upon its structure and nature.<sup>7,9,10</sup> Therefore, multiple factors such as dimer formability, dimeric structure, and inclusion by  $\gamma$ -CD must be important in determining sensitivity in this kind of molecular recognition. The present inclusion system can be regarded as a new and multifactorial model for the biological systems of molecular recognition.

(9) (a) Yokoi, H.; Takeuchi, A.; Yamada, S. *Bull. Chem. Soc. Jpn.* **1985**, *58*, 2990. (b) Yokoi, H.; Takeuchi, A.; Yamada, S. *Bull. Chem. Soc. Jpn.* **1990**, *63*, 1462 and references cited therein.

(10) (a) Yokoi, H.; Chikira, M. *J. Am. Chem. Soc.* **1975**, *97*, 3975. (b) Chikira, M.; Yokoi, H. *J. Chem. Soc., Dalton Trans.* **1977**, 2344.

Another interesting point of the present inclusion phenomena is concerned with the active transport or concentration of substances. Cu-PyC can form a 1:1 inclusion complex with  $\alpha$ -CD but a more stable 2:1 one with  $\gamma$ -CD. This fact gives us an idea about a chemical substance transport system in which Cu-PyC migrates to an adjacent area of  $\alpha$ -CD and then to the next area of  $\gamma$ -CD. Furthermore, there may exist some unknown host compound capable of forming a much more stable inclusion complex with some higher polymeric species of Cu-PyC. A certain system composed of the CDs and the above unknown host compound is considered as a new model for the active transport or concentration of substances in biological systems. This model is also based on high sensitivity in molecular recognition, as mentioned above.

## Ligand Spin Densities in Blue Copper Proteins by Q-Band $^1\text{H}$ and $^{14}\text{N}$ ENDOR Spectroscopy

Melanie M. Werst, Clark E. Davoust, and Brian M. Hoffman\*

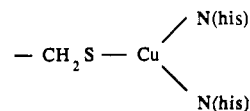
Contribution from the Department of Chemistry, Northwestern University, Evanston, Illinois 60208. Received May 31, 1990

**Abstract:** The type 1 or blue copper centers of poplar plastocyanin (*Populus nigra var italica*), azurin (*Pseudomonas aeruginosa*), stellacyanin (*Rhus vernicifera*), and type 2 reduced fungal (*Polyporus versicolor*) and tree (*R. vernicifera*) laccase have been studied by Q-band (35 GHz) ENDOR spectroscopy. At this microwave frequency the  $^1\text{H}$  and  $^{14}\text{N}$  resonances occur in completely distinct radio-frequency ranges, and this has enabled us to study them individually for the first time. Each protein exhibits strongly coupled methylene protons of cysteine with isotropic hyperfine splittings in the range 16–31 MHz. The measurements indicate that the geometry of the Cu-cys linkage as measured by the  $\text{H}^\beta\text{-C}^\beta\text{-S-Cu}$  dihedral angles is remarkably similar in all these proteins,  $-58^\circ \leq \theta(\text{H}^\beta) \leq -50^\circ$ . With one exception, all the proteins have a similar, large total spin density on sulfur; fungal laccase appears to have a larger value but rather may differ slightly in structure. The Cu-bound nitrogens of the two histidine ligands of plastocyanin give a single  $^{14}\text{N}$  resonance with isotropic coupling ( $A^{\text{N}} \sim 22$  MHz) and thus the Cu-N bonds appear effectively equivalent although they differ metrically. In contrast, azurin, stellacyanin, and fungal laccase exhibit  $^{14}\text{N}$  signals with isotropic hyperfine interactions from two inequivalent histidyl nitrogen ligands. We estimate the sum of the spin densities on N to be  $\geq 0.1$  and the overall spin density on ligands to be over 50%. The  $^{14}\text{N}$  ENDOR of the similar site of tree laccase requires that it be unlike any of the other type 1 centers studied, with at least one  $^{14}\text{N}$  ligand whose hyperfine tensor is highly anisotropic. Together, the  $^1\text{H}$  and  $^{14}\text{N}$  data suggest that the single-site proteins and the laccases fall into different subclasses. The advantages of the Q-Band ENDOR technique over alternate methods of determining ligand superhyperfine couplings also are discussed.

### Introduction

The type 1 sites of blue copper proteins have unusual optical and magnetic properties which include intense ( $\epsilon = 3500\text{--}6000$   $\text{M}^{-1}\text{cm}^{-1}$ ) absorption bands in the visible region of the spectrum ( $\lambda = 600\text{--}625$  nm), an approximately axial EPR spectrum with very low hyperfine splitting constant ( $A_{\parallel} \approx 0.006$   $\text{cm}^{-1}$ ), and relatively high reduction potentials.<sup>1</sup> Despite the great effort made toward understanding the spectral features and the associated electronic structure of these sites, they continue to be of interest because they are so different from ordinary tetrahedral or square-planar  $\text{Cu}^{2+}$  complexes. Crystal structures<sup>2</sup> have been reported for the two single-site blue copper electron-transfer proteins, plastocyanin<sup>2a</sup> and azurin.<sup>2b</sup> In both cases, the  $\text{Cu}^{2+}$  ion has three strongly bonded ligands, the thiolate sulfur of a cysteine and the imidazole nitrogens of two histidines. The primary coordination geometry of  $\text{Cu}^{2+}$  in the two proteins is very similar,

with unequal Cu-N1 and Cu-N2 bond distances and unequal S-Cu-N1 and S-Cu-N2 bond angles,<sup>3</sup> and can be schematically represented as follows



The structure of azurin from *Pseudomonas aeruginosa* (2.7 Å) has not yet been fully refined, but present coordinates<sup>2c</sup> are not inconsistent with the results for azurin from *Azotobacter denitrificans*.

Electron-nuclear double resonance (ENDOR) spectroscopy provides detailed information about the coordination sphere of

(1) (a) Ainscough, E. W.; Bingham, A. G.; Brodie, A. M.; Ellis, W. R.; Gray, H. C.; Loehr, T. M.; Plowman, J. E.; Norris, G. E.; Baker, E. N. *Biochemistry* **1987**, *26*, 71–82. (b) Gray, H. B.; Solomon, E. I. In *Copper Proteins*; Spiro, T. G., Ed.; Wiley: New York, 1981; Vol. 3, pp 1–39.

(2) (a) Guss, J. M.; Freeman, H. C. *J. Mol. Biol.* **1983**, *169*, 526–563. (b) Norris, G. E.; Anderson, B. F.; Baker, E. N. *J. Am. Chem. Soc.* **1986**, *108*, 2784–2785. (c) Adman, E. T.; Sieker, L. C.; Jensen, L. H.: coordinates deposited (1980) with Brookhaven Protein Data Bank, Brookhaven National Laboratory, Upton, New York 11973.

(3) (a) The most recent crystallographic coordinates of plastocyanin are the result of a 1.33-Å refinement (Guss, J. M.; Freeman, H. C., personal communication). They give a short, 1.91 Å, Cu-N(1) bond length and a S(cys)-Cu-N(1) bond angle of 132°. The other coordinated nitrogen has a relatively long bond, 2.07 Å, with a S(cys)-Cu-N(2) bond angle of 126°. The Cu-ligand bond distances and bond angles obtained from the high-resolution structure of *A. denitrificans* azurin are quite similar: Cu-N(1), 1.96 Å; Cu-N(2), 2.06 Å; N(1)-Cu-S, 137°; N(2)-Cu-S, 119° (ref 2b). (b) The  $\text{Cu}^{2+}$  ion of plastocyanin has in addition a weaker interaction with methionine sulfur; that of the azurin has a methionine sulfur and a main chain carbonyl oxygen (from glycine) that form significantly weaker interactions in axial positions, completing an axially elongated trigonal bipyramid.

protein-bound metal centers. A previous X-band ENDOR study of the  $^1\text{H}$ ,  $^{14}\text{N}$ , and  $^{63,65}\text{Cu}$  resonances of the type 1 copper blue centers of azurin, plastocyanin, stellacyanin, and type 2 reduced tree and fungal laccases showed that the coordination environment of Cu in all these centers is broadly similar, with strongly coupled proton resonances ( $A^{\text{H}} \sim 20\text{--}30\text{ MHz}$ ) from methylene protons of the coordinated cysteinyl mercaptide,  $^{14}\text{N}$  resonances from at least one nitrogen ligand, and resonances from  $^{63,65}\text{Cu}$  in the range 60–190 MHz.<sup>4</sup> In this study, slight differences in the ENDOR spectra taken with two different microwave X-band frequencies, 9.6 and 11.6 GHz, were used to assign  $^{14}\text{N}$  and  $^1\text{H}$  signals. However, only partial success was achieved in distinguishing  $^1\text{H}$  and  $^{14}\text{N}$  resonances because they are inextricably overlapped in the 0–40 MHz range, and thus detailed analyses were impossible.

We have now reinvestigated the type 1 copper centers of poplar plastocyanin (*Populus nigra var italica*), azurin (*Pseudomonas aeruginosa*), stellacyanin (*Rhus vernicifera*), and type 2 reduced fungal (*Polyporus versicolor*) and tree laccase (*R. vernicifera*) using Q-band (35 GHz) ENDOR spectroscopy. The increase of microwave frequency from X-band ( $\sim 9\text{ GHz}$ ) to Q-band (35 GHz) shifts the  $^1\text{H}$  ENDOR signal to high radio frequency and gives complete spectral separation of the  $^{14}\text{N}$  and  $^1\text{H}$  resonances, which thus can be analyzed in detail to give estimates of the spin densities on all three strongly coordinated ligands and of the dihedral angles of the cysteinyl  $\beta$ -protons relative to the  $\text{C}^\beta\text{--S--Cu}$  plane. Advantages of the Q-band ENDOR technique over alternate methods of determining ligand superhyperfine coupling are discussed.

### Experimental Section

**Materials.** Bean plastocyanin, stellacyanin, azurin, and type 2 reduced fungal and tree laccase were prepared as described in the previous X-band study.<sup>4</sup> X-band samples were thawed on ice and transferred immediately to Q-band tubes. EPR measurements indicate that negligible amounts of type 2  $\text{Cu}^{2+}$  had formed by oxidation during transfer of laccase samples.

**ENDOR Measurements.** ENDOR spectra were recorded on a Varian Associates E-109 spectrometer as described previously<sup>5a</sup> using an E-110 microwave bridge for Q-band (35 GHz).<sup>5b</sup> The first-order ENDOR spectrum of a nucleus ( $J$ ) of spin  $I$  for a single orientation of a paramagnetic center consists, in principle, of  $2I$  transitions at frequencies given by eq 1. Here  $A^J$  and  $P^J$  are the angle-dependent hyperfine and

$$\nu_{\pm} = A^J/2 \pm \nu_J + (3P^J/2)(2m - 1) \quad (1)$$

quadrupole coupling constants, respectively, which are molecular parameters and independent of the spectrometer microwave frequency,<sup>6</sup> and  $\nu_J$  is the nuclear Larmor frequency,  $\nu_J = g_J\beta_J H$ . For a set of equivalent  $^{14}\text{N}$  ( $I = 1$ ) nuclei ( $A^{\text{N}}/2 > \nu_{\text{N}} > 3P^{\text{N}}/2$ ), eq 1 in principle describes a four-line pattern centered at  $A^{\text{N}}/2$  consisting of a Larmor split doublet further split by the quadrupole term. Because the center of the  $^{14}\text{N}$  pattern is determined by a molecular parameter,  $A^{\text{N}}/2$ , the center of this pattern does not change with the spectrometer frequency. A set of magnetically equivalent protons ( $^1\text{H}$ ,  $I = 1/2$ ) gives a hyperfine-split doublet of ENDOR transitions ( $\nu_{\pm}$ ) whose center is determined by the free-proton Larmor frequency,

$$\nu_{\pm} = \nu_{\text{H}} \pm A^{\text{H}}/2 \quad (2)$$

$\nu_{\text{H}} = (g_{\text{H}}\beta_{\text{H}}/\beta_{\text{e}})(\nu(\text{M})/g_{\text{obs}})$  which varies with the EPR spectrometer frequency and the observing  $g$  value,  $g_{\text{obs}}$ . For fixed  $g_{\text{obs}}$  the center of the proton resonance pattern shifts in proportion to the microwave frequency,  $\nu(\text{M})$ . Because of this, it is sometimes convenient to plot  $^1\text{H}$  ENDOR spectra as  $\delta\nu = \nu - \nu_{\text{H}}$  to give them a common center.

The X-band EPR spectra of the type 1 centers of the blue copper proteins appear to have axial symmetry, but at Q-band small rhombic

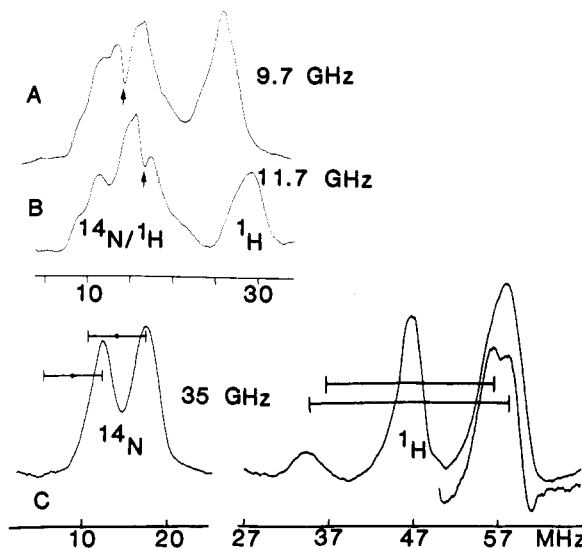


**Figure 1.**  $^1\text{H}$  and  $^{14}\text{N}$  X-band ENDOR of azurin near  $g_{\parallel}$  at (A) 9.6, (B) 11.7, and (C) 35.2 GHz. Conditions:  $T = 2\text{ K}$ ; microwave power  $2\ \mu\text{W}$  (A, B),  $50\ \mu\text{W}$  (C); 100 kHz field modulation 0.3 mT (inset, 0.1 mT modulation amplitude); radio frequency sweep 2.5 MHz/s. The arrows indicate the proton Larmor frequency at each microwave frequency.

splittings are observed. The  $g$  values are the following: azurin,  $g_{\parallel} = 2.263$ ,  $g_{1,2} = 2.03$ ,  $2.06$ ;<sup>7</sup> plastocyanin,  $g_{\parallel} = 2.226$ ,  $g_{1,2} = 2.028$ ,  $2.053$ ;<sup>8</sup> stellacyanin,  $g_{\parallel} = 2.282$ ,  $g_{1,2} = 2.018$ ,  $2.075$ ;<sup>9</sup> fungal laccase,  $g_{\parallel} = 2.19$ ,  $g_{1,2} = 2.033$ ,  $2.051$ ;<sup>10</sup> tree laccase,  $g_{\parallel} = 2.30$ ,  $g_{1,2} = 2.03$ ,  $2.06$ .<sup>9b,10</sup> When discussing  $^1\text{H}$  and  $^{14}\text{N}$  ENDOR spectra taken at Q-band it is acceptable to ignore the  $^{63,65}\text{Cu}$  hyperfine splittings because of the large field dispersion from  $g$  anisotropy and to denote an observing field in terms of a  $g$  value. The single-crystal-like ENDOR spectra shown in the figures have all been taken at  $g_{\parallel}$ .

### Results

#### Comparison of X- and Q-Band $^1\text{H}$ and $^{14}\text{N}$ ENDOR Spectra.

Parts A and B of Figure 1 show the single-crystal-like ( $g_{\parallel}$ ) ENDOR spectrum of the type 1  $\text{Cu}^{2+}$  center azurin taken at 9.6 and 11.7 GHz, respectively. These X-band spectra represent a complicated overlap of resonances from protons and nitrogens and hence their interpretation is very difficult. However, slight differences in resonant frequencies at the two microwave frequencies were used previously<sup>4</sup> to assign the  $^{14}\text{N}$  and  $^1\text{H}$  features. The proton Larmor frequency is  $\nu_{\text{H}} \sim 14\text{ MHz}$  in Figure 1A, but  $\nu_{\text{H}} \sim 17\text{ MHz}$  in Figure 1B. Comparison of the spectra clearly indicates that the well-resolved, intense high-frequency signal at ca. 26 MHz in Figure 1A shifts to ca. 29 MHz at the higher microwave frequency of Figure 1B and thus can be assigned to the  $\nu_{+}$  feature of a strongly coupled proton(s) with  $A^{\text{H}} = 24\text{ MHz}$  (eq 2).

In contrast,  $^{14}\text{N}$  resonances should show no shift between Figure 1A (9.6 GHz) and Figure 1B (11.7 GHz). The center of a  $^{14}\text{N}$  pattern is given by the molecular parameter  $A^{\text{N}}/2$ , which is independent of the spectrometer microwave frequency; furthermore at these two microwave frequencies  $\nu_{\text{N}}$  corresponds to 1.0 and 1.1 MHz, respectively, and hence the change in the splitting of the  $\nu_{-}$  and  $\nu_{+}$   $^{14}\text{N}$  resonances ( $2\nu_{\text{N}} \sim 2\text{ MHz}$ ) is undetectable. The signals in the range 7–22 MHz are poorly resolved, and it is difficult to distinguish those due to weakly coupled protons and those from nitrogen. However, it was argued that a poorly resolved feature centered at 9 MHz and ca. 2 MHz in width is seen in both parts A and B of Figure 1, and this was assigned to  $^{14}\text{N}$  ( $A^{\text{N}} \sim$

(4) Roberts, J. E.; Cline, J. F.; Lum, V.; Freeman, H. C.; Gray, H. B.; Peisach, J.; Reinhammar, B.; Hoffman, B. M. *J. Am. Chem. Soc.* **1984**, *106*, 5324–5330.

(5) (a) Venters, R. A.; Nelson, M. J.; McLean, P.; True, A. E.; Levy, M. A.; Hoffman, B. M.; Orme-Johnson, W. H. *J. Am. Chem. Soc.* **1986**, *108*, 3487–3498. (b) Gurbiel, R. J.; Batie, C. J.; Sivaraja, M.; True, A. E.; Fee, J. A.; Hoffman, B. M.; Ballou, D. P. *Biochemistry* **1989**, *28*, 4861–4871.

(6) (a) Abragam, A.; Bleaney, B. *Electron Paramagnetic Resonance of Transition Ions*; Clarendon: Oxford, 1970. (b) Atherton, N. M. *Electron Spin Resonance*; Wiley: New York, 1974. (c) Hoffman, B. M.; Gurbiel, R. J.; Werst, M. M.; Sivaraja, M. *Advanced EPR*; Hoff, A. J., Ed.; Elsevier: Amsterdam; pp 541–592.

(7) Groenvelde, C. M.; Aasa, R.; Reinhammar, B.; Canters, G. W. *J. Inorg. Biochem.* **1987**, *31*, 143–154.

(8) Penfield, K. W.; Gay, R. R.; Himmelwright, R. S.; Eichman, N. C.; Norris, V. A.; Freeman, H. C.; Solomon, E. I. *J. Am. Chem. Soc.* **1981**, *104*, 4519–4529.

(9) (a) Malmström, B. G.; Reinhammar, B.; Vänngård, T. *Biochim. Biophys. Acta* **1970**, *205*, 48–57. (b) Reinhammar, B. *J. Inorg. Biochem.* **1981**, *15*, 24–28.

(10) Reinhammar, B. In *Copper Proteins and Copper Enzymes*; Lontie, R., Ed.; CRC: Boca Raton, 1984; Vol. 3, pp 1–33.

**Table I.**  $^1\text{H}$  and  $^{14}\text{N}$  Isotropic Hyperfine Coupling Constants<sup>a</sup> (MHz) of Blue Copper Centers

|                             | $^1\text{H}^b$                       |                                     |                              |                   |                       | $^{14}\text{N}^c$ |                 |
|-----------------------------|--------------------------------------|-------------------------------------|------------------------------|-------------------|-----------------------|-------------------|-----------------|
|                             | $A^{\text{H}19}(\text{H}^{\beta 2})$ | $A^{\text{H}2}(\text{H}^{\beta 1})$ | $\theta(\text{H}^{\beta 2})$ | $[B\rho_s]$ , MHz | $\rho_s^{\text{rel}}$ | $A^{\text{N}1}$   | $A^{\text{N}2}$ |
| plastocyanin                | 27                                   | 16                                  | -50                          | 44                | 1.0                   | 22                | 22 <sup>d</sup> |
| azurin                      | 23                                   | 18                                  | -54                          | 43                | 0.96                  | 27                | 17              |
| stellacyanin <sup>e</sup>   | 20                                   | 20                                  | -58                          | 42                | 0.94                  | 33                | 17              |
| fungal laccase <sup>f</sup> | 31                                   | 25                                  | (-55)                        | (59)              | (1.33)                | 36                | 23              |
| tree laccase                | 25                                   | 19                                  | -54                          | 46                | 1.04                  | 40 <sup>g</sup>   | 33              |

<sup>a</sup> Measured in the  $g_{\parallel}$  region of the EPR spectrum. All hyperfine interactions with the exception of the  $^{14}\text{N}$  interaction of N1 of tree laccase are roughly isotropic (see text). <sup>b</sup> The quantities  $[B\rho_s]$  and  $\theta(\text{H}^{\beta 2})$  are defined in the text and calculated with eq 4 as parametrized from  $\theta(\text{H}^{\beta 2})$  and the  $A^{\text{H}i}$  of plastocyanin;  $\theta(\text{H}^{\beta 1}) = \theta(\text{H}^{\beta 2}) + 116^\circ$ ;  $\rho_s^{\text{rel}} = [B\rho_s]/[B\rho_s]_{\text{plastocyanin}} \cong \rho_s/\rho_{\text{plastocyanin}}$ . <sup>c</sup> The spin density on the nitrogen discussed in the text is obtained from the ratio of the  $^{14}\text{N}$  hyperfine couplings of the protein and that for Cu(tetraphenylporphyrin);  $A_{\text{iso}}[\text{Cu}(\text{tetraphenylporphyrin})] \sim 0.1$ .<sup>29</sup> <sup>d</sup> See text for the assignment of equivalent nitrogens. <sup>e</sup> See text and footnote 14 for assignment of equivalent protons and inequivalent nitrogens. <sup>f</sup> Parentheses around derived values reflect a probability that the plastocyanin parametrization of eq 4 may not apply. <sup>g</sup> Tensor components,  $A_{3,2,1} = [32, 42, 47]$  MHz. See text for discussion of assignments.

18 MHz). Any additional nitrogen resonances appearing at  $A^{\text{N}}/2 \sim 13$ –18 MHz would be obscured by the signals from weakly coupled protons centered at  $\nu_{\text{H}}$ .

Such difficulties in making assignments arose for each blue copper protein.<sup>4</sup> Furthermore, the  $^{14}\text{N}$  signals that were assigned at X-band could not be analyzed in detail by measuring their dependence on the observing field. Hence, we have now repeated these measurements at Q-band microwave frequency. As seen in Figure 1C the  $^1\text{H}$  and  $^{14}\text{N}$  resonances are completely separated, and thus they can be unambiguously assigned and analyzed.

**$^1\text{H}$  Q-Band ENDOR.** Figure 2 shows the single-crystal-like  $^1\text{H}$  ENDOR spectrum taken at  $g_{\parallel}$  for each of the type 1 copper proteins. The spectra are centered at  $\nu_{\text{H}} \sim 47$  MHz with the  $\nu_+$  and  $\nu_-$  features split by the hyperfine coupling constant,  $A_{\text{H}}$ . Because of the details of the spin cross-relaxation, the  $\nu_+$  branch of all the  $^1\text{H}$  spectra shown here is considerably more intense than the  $\nu_-$  branch; in the case of plastocyanin (Figure 2A), the  $\nu_-$  features are too weak to be detected. All the proteins display signals that are associated with weakly coupled protons,  $A^{\text{H}} \leq 6$  MHz. These protons are from coordinating groups such as the imidazole of histidine, with possible contributions from nearby, noncoordinating residues. In each case, strongly coupled protons also are observed, with hyperfine splittings in the range  $A^{\text{H}} \sim 15$ –31 MHz. For stellacyanin, Figure 2C, only one such strongly coupled proton doublet is observed in this range, plus a partially resolved proton resonance with intermediate coupling,  $A^{\text{H}} \sim 8$  MHz. For all other type 1 centers there are two strongly coupled proton doublets. The hyperfine splittings are summarized in Table I. For each protein, the Q-band proton ENDOR spectrum changes little with field position,<sup>11</sup> which indicates that the hyperfine couplings are effectively isotropic (10–20% anisotropy).

Given the X-ray crystallographic identification of the three strongly coordinating Cu ligands in plastocyanin and azurin (see structure above), we assign the strongly coupled protons for these proteins to the  $-\text{CH}_2-\text{S}^-$  chain of the cysteine coordinated to Cu. Comparison to earlier ENDOR studies<sup>12</sup> of  $[\text{Cu}(\text{Im})_4]^{2+}$  shows that the protons associated with  $\text{Cu}^{2+}$ -bound imidazole in the type 1 centers must give hyperfine couplings,  $A^{\text{H}} \ll 5$  MHz. For organic sulfur radicals, such large isotropic couplings are attributed to spin-polarization of the S–C and C–H bonds by spin density on the sulfur, in which case they normally obey a relationship of the form<sup>6b,13a</sup>

$$A^{\text{H}1} = B[\cos^2 \theta] \sigma_s, \quad A^{\text{H}2} = B[\cos^2 (\theta - 2\pi/3)] \sigma_s \quad (3)$$

where  $B \sim 100$  MHz,  $\sigma_s$  is the  $\pi$  spin density on the sulfur, and  $\theta$  is the dihedral angle between the  $\pi$ -orbital on S and the C–H1 bond. In the case of the mercaptide sulfur bound to the  $\text{Cu}^{2+}$  ion, spin density on sulfur would have both  $\sigma$  and  $\pi$  contributions and for fixed  $\text{C}_\text{B}-\text{S}-\text{Cu}$  angle we might expect the proton hyperfine couplings to depend on the dihedral angle between the

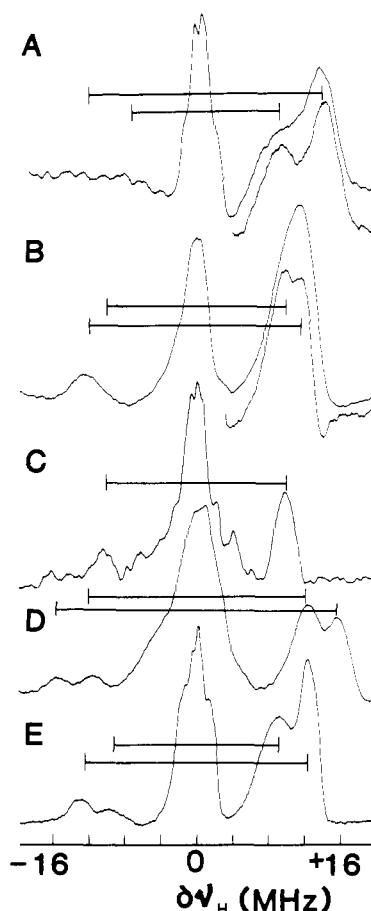


**Figure 2.**  $^1\text{H}$  Q-band spectra at  $g_{\parallel}$  plotted as  $\delta\nu = \nu - \nu_{\text{H}}$ : (A) plastocyanin,  $g = 2.198$ ,  $H = 1.11$  T, 34.15 GHz, modulation amplitude 0.32 mT (inset: modulation amplitude, 0.2 mT); (B) azurin,  $g = 2.262$ ,  $H = 1.113$  T, 35.2 GHz, 0.2 mT modulation amplitude (inset 0.1 mT modulation amplitude); (C) stellacyanin,  $g = 2.27$ ,  $H = 1.11$  T, 35.2 GHz, 0.4 mT modulation amplitude; (D) type 2 reduced fungal laccase,  $g = 2.2$ ,  $H = 1.15$  T, 35.27 GHz, 0.8 mT modulation amplitude; (E) type 2 reduced tree laccase,  $g = 2.3$ ,  $H = 1.11$  T, 35.25 GHz, modulation amplitude 0.4 mT. For all spectra shown  $T = 2$  K, modulation frequency 100 KHz, radio frequency scan rate 6 MHz/s, and rf power 10 W. Each spectrum is the average of ca. 90 scans.

$\text{H}^i-\text{C}^\beta-\text{S}-\text{Cu}$  dihedral angle,  $\theta(\text{H}^{\beta i})$  ( $i = 1, 2$ ;  $\theta(\text{H}^{\beta 2}) \sim \theta(\text{H}^{\beta 1}) - 2\pi/3$ ), and the total spin density on sulfur,  $\rho_s$ , through a more general expression

$$A^{\text{H}i} = [B \cos^2 \theta_i + C] \rho_s; \quad i = 1, 2 \\ = [\cos^2 \theta_i + C/B] [B\rho_s] \quad (4)$$

As a basis for discussing the present data, we have parametrized this expression through use<sup>13b</sup> of the high-precision structure of plastocyanin,<sup>3a</sup> where it is found that  $\theta(\text{H}^{\beta 1}) = +66^\circ$  and  $\theta(\text{H}^{\beta 2}) = -50^\circ$ . Inspection of eq 4 shows that we can identify  $\text{H}_1$  with

(11) Wersl, M. Ph.D. Thesis, Northwestern University, 1990.  
 (12) Van Camp, H. L.; Sands, R. H.; Fee, J. A. *J. Chem. Phys.* **1981**, *75*(5), 2098–2107.  
 (13) (a) Gordy, W. *Theory and Applications of Electron Spin Resonance*; Wiley: New York, 1980. (b) We thank a referee for suggesting parametrization could be achieved through reference to the plastocyanin structure.

$H^{\beta 2}$  and the reverse; introduction of the  $A^{\text{H}i}$  for plastocyanin from Table I gives  $[B\rho_s] = 44$  MHz and  $[C/B] = 0.2$ . To appreciate these values, we note that the assumption that  $B \sim 100$  MHz,<sup>13a</sup> which probably has an uncertainty of more than  $\pm 20\%$ , would give  $\rho_s = 0.44$ . If we assume that the metrical result  $\{\theta(H^{\beta 1}) - \theta(H^{\beta 2})\} = 116^\circ$  and the fitting constant  $[C/B]$  are invariant among the type I sites, then eq 4 and the hyperfine couplings in Table I can be used to calculate  $\theta(H^{\beta 2})$  (and of course  $\theta(H^{\beta 1})$ ) and the product  $[B\rho_s]$  for each protein. It is easy to show that ca. 20% variation in  $[C/B]$  causes negligible change in  $\theta$  and less than a 20% change in  $[B\rho_s]$  and thus in the value of  $\rho_s$  calculated by using an assumed value of  $B$ .

Table I gives values of  $\theta(H^{\beta 2})$  and  $[B\rho_s]$  for each protein studied. The only apparent difficulty in assignment is with stellacyanin, where only one strongly coupled doublet is observed. As its hyperfine coupling is roughly the average of the two for plastocyanin, we take this to be the case where  $\theta(H^{\beta 1}) = -\theta(H^{\beta 2}) = 58^\circ$  and  $A^{\text{H}1} = A^{\text{H}2}$ . With this assignment,<sup>14a</sup> then for all the proteins eq 4 gives a small spread in angles,  $-58^\circ \leq \theta(H^{\beta 2}) \leq -50^\circ$ , a remarkably small spread; indeed there are only three different values,  $-58^\circ$ ,  $-(54-55^\circ)$ ,  $-50^\circ$ . This analysis clearly suggests that the geometry of the cysteinyl-Cu linkage is remarkably well conserved. For all proteins *except* fungal laccase  $44 \leq [B\rho_s] \leq 46$  MHz. Thus, the spin density on sulfur, with one exception, also is conserved; for concreteness, if  $B \sim 100$  MHz then  $\rho_s \sim 0.45$ . The value  $[B\rho_s] = 59$  MHz for the fungal protein indicates it to be quite distinct from the others.

**<sup>14</sup>N Q-Band ENDOR.** (a) **Plastocyanin, Azurin, and Stellacyanin.** The low-frequency portions ( $\nu < 30$  MHz) of the  $g_1$  single-crystal-like spectra for these single-site copper proteins (Figure 3A-C) show intense resonances that we assign to  $\nu_+$  for nitrogen coordinated to Cu. The  $\nu_-$  partners at lower frequency are too weak to be detected; this low relative intensity parallels that for the  $\nu_-$  peaks of the strongly coupled protons of all the type I centers (Figure 2) (and for the strongly coupled nitrogen (N2) of fungal laccase (Figure 3D)). None of these Q-band spectra show resolved quadrupole splittings for <sup>14</sup>N ( $I = 1$ ), consistent with other results: <sup>14</sup>N quadrupolar splittings have not been observed for the nitrogen of histidine that is directly coordinated to copper in <sup>12</sup> [Cu(lm)<sub>4</sub>]<sup>2+</sup>, or in the Cu<sub>A</sub> site of cytochrome oxidase.<sup>15</sup>

The  $g_1$  <sup>14</sup>N ENDOR spectra of azurin and stellacyanin (Figure 3, parts B and C, respectively) show two intense peaks that we assign to the  $\nu_+$  resonances of two inequivalent <sup>14</sup>N ligands. The <sup>14</sup>N Q-band ENDOR spectra taken at selected  $g$  values across the epr envelope<sup>11</sup> indicate that the hyperfine splittings of N1 and N2 are roughly isotropic (10% anisotropy), with  $A^{\text{N}1} = 27$  MHz and  $A^{\text{N}2} = 17$  MHz for azurin and  $A^{\text{N}1} = 33$  MHz and  $A^{\text{N}2} = 17$  MHz for stellacyanin.<sup>14b</sup>

For poplar plastocyanin there is a single <sup>14</sup>N  $\nu_+$  peak whose Q-band field dependence<sup>11</sup> indicates that the <sup>14</sup>N hyperfine coupling also is roughly isotropic,  $A^{\text{N}} \sim 22$  MHz. Because the crystal structure shows that there are two histidine ligands, the observation of a single <sup>14</sup>N resonance implies that the nitrogens are magnetically equivalent,  $A^{\text{N}1} \sim A^{\text{N}2} \sim 22$  MHz. The alternative

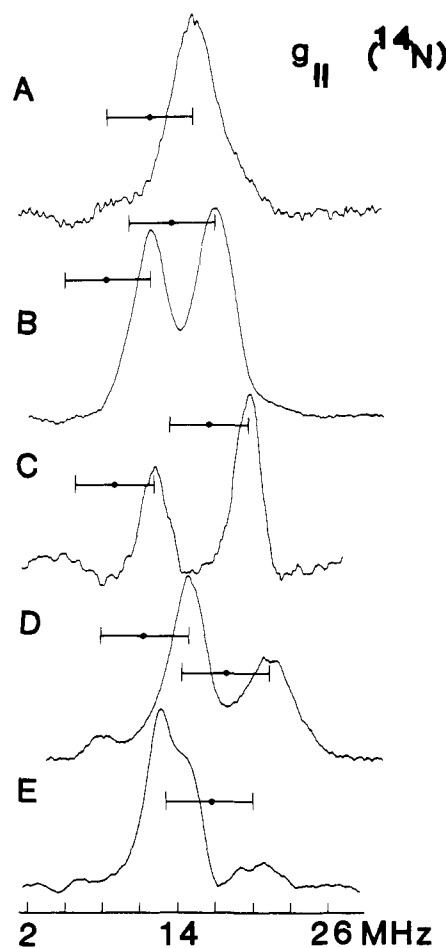


Figure 3. <sup>14</sup>N Q-band spectra at  $g_1$  of (A) plastocyanin:  $g = 2.226$ ,  $H = 1.133$  T, 34.15 GHz, 0.8 mT modulation amplitude; (B) azurin,  $g = 2.262$ ,  $H = 1.113$  T, 35.2 GHz, 0.6 mT modulation amplitude; (C) stellacyanin,  $g = 2.28$ ,  $H = 1.104$  T, 35.2 GHz, 0.8 mT modulation amplitude; (D) type 2 reduced fungal laccase,  $g = 2.19$ ,  $H = 1.15$  T, 35.27 GHz, 0.8 mT modulation amplitude; (E) type 2 reduced tree laccase,  $g = 2.3$ ,  $H = 1.089$  T, 35.25 GHz. Other conditions are as described in Figure 2.

would be a second nitrogen with an unobservably small hyperfine coupling. However, it is unlikely that we could fail to detect a coordinated nitrogen: we easily detect<sup>15a</sup> couplings as low as  $A^{\text{N}} = 6$  MHz in the case of Cu<sub>A</sub> of *Thermus* cytochrome  $c_{1aa_3}$  from *Thermus thermophilus*. As further support for this assignment we note that the hyperfine coupling for the single plastocyanin <sup>14</sup>N resonance is the average for the two couplings for azurin (Table I).

Considering that the structures of both poplar plastocyanin and azurin show two different Cu-N bond distances,<sup>2,3</sup> it is surprising that the two histidine nitrogens are magnetically equivalent in plastocyanin but inequivalent in azurin. The spin density on each nitrogen ligand depends on both the Cu-N distance and the angle made by the Cu-N bond and the adjacent lobe of the  $d(x^2-y^2)$  orbital of the Cu ion. Apparently the net balance of these parameters is different in plastocyanin and azurin, but only detailed calculations are likely to be able to reconcile these results with the coordination geometry of Cu.

The crystal structure of stellacyanin, which contains no methionine<sup>16</sup> has not yet been solved. However, there is evidence<sup>17-19</sup> that this type I center has the same strongly coordinated ligands,

(16) Bergman, C.; Gandvik, E.-K.; Nyman, P. O.; Strid, L. *Biochem. Biophys. Res. Commun.* **1977**, *77*, 1052-1059.

(17) Lappin, A. G. *Met. Ions Biol. Syst.* **1981**, *13*, 15-71.

(18) Feilters, M. C.; Dahlin, S.; Reinhammar, B. *Biochim. Biophys. Acta*, **1988**, *955*, 250-260.

(19) Dahlin, S.; Reinhammar, B.; Ångström, J. *Biochemistry* **1989**, *28*, 7224-7233.

(14) (a) The alternate assignment of the  $A^{\text{H}} \sim 8$  MHz coupling of stellacyanin (Figure 2C) to the second methylene proton of a cysteine ligand leads to  $\theta(H^{\beta 2}) = 44^\circ$ , which would indicate that stellacyanin is quite different from azurin and plastocyanin. Thus, the coupling  $A^{\text{H}} \sim 8$  MHz is provisionally associated with the ligand that replaces the methionine present in azurin and plastocyanin. (b) The spacing of the two <sup>14</sup>N peaks for stellacyanin (Figure 3C) is sufficiently close to  $2\nu_{\text{N}}$  to suggest the alternative assignment of a single type of nitrogen with  $A^{\text{N}} \sim 32$  MHz. On the basis of the previous X-band data (ref 4), Q-band field dependence (ref 11), and the equal intensities, we adopt the assignment in the text. Data at 24 GHz will eliminate uncertainties.

(15) (a) Q-band studies of Cu<sub>A</sub> of cytochrome *c* oxidase and cytochromes  $c_{1aa_3}$  and  $ba_3$  from *Thermus thermophilus*: Werst, M.; Zimmerman, B.; Fee, J. A.; Hoffman, B. M. Manuscript in preparation. (b) Quadrupole interactions are resolved in a single-crystal ENDOR study of Cu-doped histidine monodeuterohydrate (ref 15c). However, the relevance of this elegant work in these instances is questionable, as the <sup>14</sup>N hyperfine coupling is quite anisotropic, unlike that seen in [Cu(lm)<sub>4</sub>]<sup>2+</sup> or most of the type I sites, or in Cu<sub>A</sub> (ref 15a). (c) Naito, L.; Sastry, D. L.; Cui, Y. U.; Sha, K.; Yu, S. X. *J. Mol. Struct.* **1989**, *195*, 361-381.

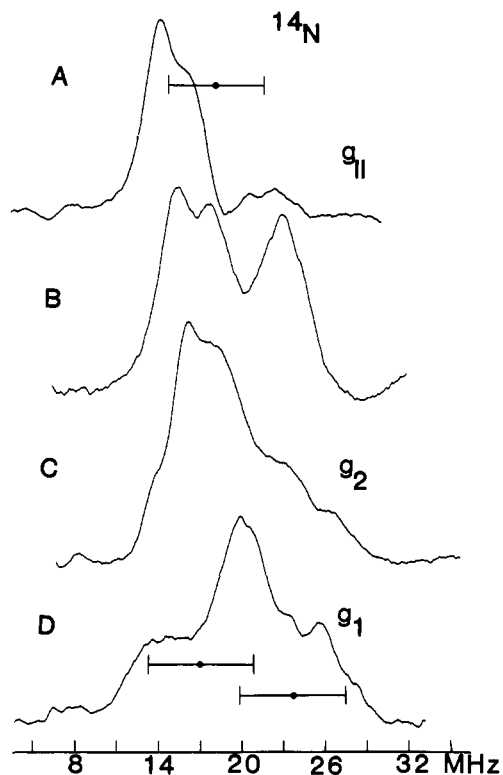


**Figure 4.** Type 2 reduced tree laccase;  $^{14}\text{N}$  ENDOR spectra of the type 1 site at selected  $g$  values: (A)  $g = 2.3$ ,  $H = 1.089$  T; (B)  $g = 2.19$ ,  $H = 1.15$  T; (C)  $g = 2.065$ ,  $H = 1.22$  T; (D)  $g = 2.03$ ,  $H = 1.241$  T. Other conditions are as described in Figure 3.

one cys and two his, as azurin and plastocyanin. The  $^{14}\text{N}$  Q-band ENDOR spectrum of stellacyanin resembles that of azurin, with resonances from two inequivalent  $^{14}\text{N}$  ligands, although the hyperfine couplings of N1 is slightly larger in the former protein. A closer resemblance of stellacyanin to azurin than plastocyanin also is observed in the cadmium NMR study of Engeseth et al.<sup>20</sup>

**(b) Fungal and Tree Laccase.** Fig 3D shows the single-crystal-like  $^{14}\text{N}$  spectrum at  $g_{\parallel}$  of the type 1  $\text{Cu}^{2+}$  center of fungal laccase. The intense peaks at 15 and 22 MHz are assigned as the  $\nu_+$  resonances of two inequivalent  $^{14}\text{N}$  ligands; in this case the low-intensity  $\nu_-$  partner of N2 actually is visible at  $\sim 8$  MHz. Again the field dependence of these peaks indicates that the hyperfine splittings are approximately isotropic,  $A^{\text{N}1} = 36$  MHz and  $A^{\text{N}2} = 23$  MHz.

The  $g_{\perp}$  ENDOR spectrum of the type 1  $\text{Cu}^{2+}$  site in tree laccase (Figure 3E) shows an intense resonance at  $\sim 13$  MHz and a very poorly resolved feature of considerably reduced intensity at a frequency higher by  $2\nu_{\text{N}} = 6.7$  MHz. We assign these to the  $\nu_+$  and  $\nu_-$  partners of a  $^{14}\text{N}$  pattern associated with a hyperfine coupling  $A^{\text{N}2}(g_{\perp}) \sim 33$  MHz. The atypically low intensity of the  $\nu_+$  feature relative to the  $\nu_-$  partner at  $g_{\perp}$  (Figure 3E) also has been observed at Q-band in the  $^{57}\text{Fe}$  resonances in the  $[\text{4Fe-4S}]^+$  cluster of aconitase,<sup>21</sup> but it is one of several characteristics that distinguishes the tree laccase type 1 site from the others; the intensity of the  $\nu_+$  feature increases considerably as the observing  $g$  value moves away from  $g_{\parallel}$  as seen at  $g = 2.2$  (Figure 4B). The  $^{14}\text{N}$  Q-band ENDOR spectra of tree laccase type 1 Cu taken at selected  $g$  values across the EPR envelope are shown in Figure 4. These can be analyzed in terms of one nitrogen ligand that has a quite anisotropic hyperfine tensor of approximately axial symmetry,  $A^{\text{N}1}_{3,2,1} = [32, 31, 47$  MHz], where the slight splittings in the  $\nu_+$  and  $\nu_-$  peaks represent resolved quadrupole splittings. However, as discussed above, quadrupole splittings typically are

not observed for the histidyl N that is bound to Cu (but see ref 15b); this, along with extensive ENDOR simulations,<sup>6c,22-24</sup> led us to prefer an interpretation in terms of two inequivalent nitrogen ligands where the hyperfine interaction of N2 is roughly isotropic ( $A \sim 33$  MHz) and that of N1 is strongly anisotropic,  $A_{3,2,1} = [32, 42, 47$  MHz]. In either case, the intensity that develops at  $\sim 26$  MHz in the spectra taken at  $g = 2.065$  (Figure 4C) and 2.03 (Figure 4D) requires that there be a strongly anisotropic  $^{14}\text{N}$  hyperfine interaction with a tensor component,  $A_1 \sim 47$  MHz. This is unique among the blue proteins studied here.

**Comparison of Q-Band ENDOR Results with Those Obtained from Alternate Techniques.** The  $^1\text{H}$  and  $^{14}\text{N}$  hyperfine coupling constants obtained from the Q-band ENDOR measurements are summarized in Table I. These results show that the use of two microwave frequencies in the X-band range<sup>4</sup> was moderately successful in distinguishing the severely overlapped  $^1\text{H}$  and  $^{14}\text{N}$  features (Figure 1). In each case the proton hyperfine coupling for H1 (Table I) was correctly identified. Of the four proteins with an H2 resonance, only those for the two laccases were resolved; the X-band H2 resonance of plastocyanin was incorrectly attributed to a very strongly coupled nitrogen ( $A^{\text{N}} \sim 49$  MHz) and the H2 resonance of azurin was not detected. The two  $^{14}\text{N}$  resonances for stellacyanin and fungal laccase, the single resonance for plastocyanin, and the N2 resonance for azurin were correctly assigned and their coupling constants were reliably obtained. At X-band, the ENDOR signal for N1 of azurin is centered at ca. 14 MHz and is totally obscured by the proton signal (Figure 1, A and B). The  $^{14}\text{N}$  resonances for tree laccase at X-band were correctly assigned, but the  $A^{\text{N}}$  values were not accurate; in retrospect, the complex  $^{14}\text{N}$  interaction described here could not possibly have been detected or fully analyzed at X-band.

Although appreciable success was achieved by use of ENDOR data obtained at two X-band frequencies,<sup>4</sup> an attempt to interpret spectra taken at a single X-band microwave frequency was not successful. Desideri et al.<sup>25</sup> disagreed with our earlier ENDOR assignments for the type 1 site of tree laccase and attributed the high-frequency resonances (20–28 MHz) in the X-band ENDOR spectrum of the type 1 center to two inequivalent nitrogens ( $A^{\text{N}1} = 54$  MHz and  $A^{\text{N}2} = 37$  MHz); they further asserted that there are no protons with  $A^{\text{H}} > 5$  MHz. The Q-band ENDOR results reported here (Figure 2E) unequivocally confirm there are two inequivalent protons with large couplings,  $A^{\text{H}1} = 25$  and  $A^{\text{H}2} = 20$  MHz, and that there is no nitrogen ligand with  $A = 54$  MHz; the latter would place the  $\nu_+$  feature at ca. 30 MHz where no intensity is seen. These erroneous assignments were apparently prompted by rejection of the large spin density on cysteinyl sulfur required by the large methylene  $^1\text{H}$  couplings verified here (Table I). Interestingly, recent calculations<sup>8,26</sup> confirm that the copper–thiolate linkage is very covalent with large spin density on sulfur and are seen below to agree well with the present results.

Multifrequency EPR techniques have been highly useful in the study of  $\text{Cu}^{2+}$  complexes<sup>27</sup> and have been applied to the type 1 Cu signal of type 2-reduced fungal laccase.<sup>28a</sup> The S-band EPR

(22) True, A. E.; Nelson, M. J.; Venters, R. A.; Orme-Johnson, W. H.; Hoffman, B. M. *J. Am. Chem. Soc.* **1989**, *111*, 1935–1943.

(23) Hoffman, B. M.; Martinsen, J.; Venters, R. A. *J. Magn. Reson.* **1984**, *59*, 110–123.

(24) Hoffman, B. M.; Martinsen, J.; Venters, R. A. *J. Magn. Reson.* **1985**, *62*, 537–542.

(25) (a) Desideri, A.; Morpurgo, L.; Agostinelli, E.; Baker, G. J.; Raynor, J. B. *Biochem. Biophys. Acta* **1985**, *831*, 8–12. (b) Although we have studied type 2 reduced tree enzyme whereas ref 25a is concerned with type 2 depleted, the essential features of the ENDOR spectra are the same. This makes it clear that the type 1 Cu site is essentially the same in both cases.

(26) (a) Penfield, K. W.; Gewirth, A. A.; Solomon, E. I. *J. Am. Chem. Soc.* **1985**, *107*, 4519–4529. (b) Gewirth, A. A.; Solomon, E. I. *J. Am. Chem. Soc.* **1988**, *110*, 3811–3819. (c) Solomon, E. I.; Gewirth, A. A.; Westmoreland, T. D. *Advanced EPR*; Hoff, A., Ed.; Elsevier: Amsterdam, 1990; pp 865–908.

(27) Hyde, J.; Froncisz, W. *Annu. Rev. Bioeng.* **1982**, *11*, 391–417.

(28) (a) Hanna, P. M.; McMullin, D. R.; Pasenkiewicz-Gierula, M.; Antholine, W. E.; Reinhammar, B. *Biochem. J.* **1988**, *253*, 561–568. (b) In this case there is no direct ENDOR evidence that type 2 depletion does not influence the type 1 Cu site. However, the results for the tree laccase (ref 25) make this unlikely.

(20) Engeseth, H. R.; McMullin, D. R.; Olivos, J. D. *J. Biol. Chem.* **1984**, *259*, 4822–4826.

(21) Werst, M.; Kennedy, M. C.; Houseman, A.; Beinert, H.; Hoffman, B. *Biochemistry* **1990**, *29*, 10533–10540.

spectrum of this protein has been simulated on the basis of contributions from two  $^1\text{H}$  and two  $^{14}\text{N}$  nuclei with  $A^{\text{H}} \sim A^{\text{N}} \sim 25$  MHz,<sup>28a</sup> although it was emphasized that the simulations are not unique; three  $^{14}\text{N}$  atoms would do as well as two  $^{14}\text{N}$  and two  $^1\text{H}$  atoms. Clearly the S-band EPR simulations are in reasonable agreement with the  $A^{\text{H}}$  and  $A^{\text{N}}$  values determined by Q-band ENDOR for the type-2 reduced fungal laccase (Table I), given the difficulty of treating couplings from four nuclei (2 protons ( $I = 1/2$ ) and 2 nitrogens ( $I = 1$ )) with resolvable hyperfine interactions of comparable magnitude.<sup>28b</sup>

### Discussion

The complete separation of  $^1\text{H}$  and  $^{14}\text{N}$  ENDOR resonances achieved at Q-band microwave frequencies has allowed us to analyze separately the  $^1\text{H}$  and  $^{14}\text{N}$  resonances of the blue copper centers. The level of detail presented here could not be obtained from a study using several X-band frequencies, much less one using a single frequency, because of the complicated overlap of  $^1\text{H}$  and  $^{14}\text{N}$  signals at X-band; neither was it possible with the highly informative multifrequency EPR technique.

The  $^1\text{H}$  ENDOR measurements indicate that the geometry of the Cu–Cys linkage as measured by the  $\text{H}^\beta\text{--C}^\beta\text{--S--Cu}$  dihedral angles (eq 4) is remarkably similar in all these proteins (Table I). Likewise, the spin-density parameter  $[B\rho_s]$  (and thus  $\rho_s$ ) is similar in all cases except fungal laccase, which stands alone. Here it might well be that the assumption of constant  $[C/B]$ , eq 4, which requires a constancy of structure, is violated. Regardless, any reasonable value for  $B$  shows that  $\rho_s$  is large ( $\rho_s \sim 0.45$  for  $B = 100$  MHz) in qualitative agreement with calculations.<sup>8,26</sup>

The  $^{14}\text{N}$  ENDOR data show that the two histidyl ligands to  $\text{Cu}^{2+}$  of plastocyanin are effectively equivalent. The hyperfine coupling value is  $\sim 1/2$  that for  $^{14}\text{N}$  coordinated to Cu in  $[\text{Cu}(\text{imidazole})_4]^{2+}$  ( $A^{\text{N}} \sim 40\text{--}42$  MHz), which serves as the reference for imidazole to  $\text{Cu}^{2+}$  in an unconstrained square-planar complex.<sup>12</sup> To achieve a semiquantitative understanding of the Cu–N bonding, we *calibrate* the spin density on an individual  $^{14}\text{N}$  in this complex by recalling that  $A^{\text{N}} \sim 47$  MHz corresponds to a total spin density of 0.1 for a single pyrrole nitrogen of Cu(tetraphenylporphyrin).<sup>29</sup> Hence, we approximate  $\rho_{\text{N}} \sim 0.09$  for a single nitrogen ligand of  $[\text{Cu}(\text{imidazole})_4]^{2+}$ . This leads to an estimate of  $\rho_{\text{N}} \sim 0.05$

for each of the two equivalent nitrogens of plastocyanin, in pleasing, if undeserved, agreement with the theoretical value<sup>5</sup> of  $\rho_{\text{N}} = 0.05$ . For azurin and stellacyanin the hyperfine splitting  $A^{\text{N}1}$  and thus the spin density on N1 is somewhat larger,  $\sim 70\%$  that in  $[\text{Cu}(\text{imidazole})_4]^{2+}$ , whereas that for N2 is only 40% of this reference value. Presumably this difference reflects respectively better and worse overlap between the  $\text{sp}^2$  orbital of N1 and N2 with the near lobe of the  $\text{Cu}^{2+}$   $d(x^2-y^2)$ . For each of these three single-site type I Cu proteins the total spin density on the three ligands is  $\rho_{\text{L}} = \rho_s + \rho_{\text{N}1} + \rho_{\text{N}2} > 0.5$ , using any reasonable value of  $B$  to estimate  $\rho_s$ , in agreement with the calculations that indicate that the odd-electron orbital has less than 50% Cu character.<sup>8,26</sup>

The type I site of fungal laccase is like those of the single-site proteins, azurin and stellacyanin, in that it is distinctly inequivalent  $^{14}\text{N}$  ligand with roughly isotropic hyperfine interactions (Table I). However, the type I center of tree laccase is unique among these blue copper proteins. First, the  $^{14}\text{N}$  isotropic hyperfine couplings for tree laccase are larger; that for N1 is essentially the same as the coupling for a nitrogen ligand in  $[\text{Cu}(\text{imidazole})_4]^{2+}$ , and that for N2 is nearly so. Even more unusual, the hyperfine tensor of N1 is anisotropic, as it is in a  $\text{Cu}^{2+}$ -doped histidine monodeuterohydrate<sup>15c</sup> and  $\text{Cu}_A$  of cytochrome *c* oxidase,<sup>15a</sup> whereas this is not true for any of the other type I sites or for  $[\text{Cu}(\text{imidazole})_4]^{2+}$ . For both types of laccase the spin density on histidine–nitrogen ligands appears greater than that for the single-site proteins and the same would be true for the total spin density,  $\rho_{\text{L}}$  (Table I). Thus, within the type I class, the  $^1\text{H}$  and  $^{14}\text{N}$  ENDOR data suggest that the single-site proteins and the laccases fall into distinctly different subclasses.

**Acknowledgment.** We thank Professors H. Freeman, H. B. Gray, J. Peisach, and B. Reinhammar for the protein samples. We thank Prof. Freeman for details of the plastocyanin crystal structure. This work has been supported by the National Institutes of Health (HL 13531) and the National Science Foundation (DBM-8907559) and benefited from the support of the Northwestern University Materials Research Center (NSF DMR 88-18599).

**Registry No.** Cu, 7440-50-8; Cys, 52-90-4; histidine, 71-00-1; laccase, 80498-15-3.

(29) Brown, T. G.; Hoffman, B. M. *Mol. Phys.* **1980**, *39*, 1073–1109.